



Influence of crystal structure on the Co^{II} diffusion behavior in the Zn_{1-x}Co_xO system

M. Peiteado^{a,*}, D. Makovec^b, M. Villegas^a, A.C. Caballero^a

^a Department of Electroceramics, Instituto de Cerámica y Vidrio, CSIC, Kelsen 5, Madrid 28049, Spain

^b Department for Materials Synthesis, Jozef Stefan Institute, Ljubljana 1000, Slovenia

ARTICLE INFO

Article history:

Received 14 May 2008

Received in revised form

4 June 2008

Accepted 8 June 2008

Available online 12 June 2008

Keywords:

ZnO

Diffusion couples

Spinel

Solid state chemistry

Magnetic semiconductors

ABSTRACT

The solid state interaction of the Zn_{1-x}Co_xO nominal system is investigated by means of diffusion couples and analysis of co-precipitated samples. The formation of a homogeneous Co:ZnO solid solution is found to be determined by the crystal structure from which Co^{II} ions diffuse into the wurtzite lattice. No diffusion is observed whenever the CoO rock-salt structure is formed from the Co^{II} precursor. On the contrary, the diffusion from the Co₃O₄ spinel phase is feasible but has a limited temperature range defined by the reduction at a high temperature of Co^{III}–Co^{II}, since this process again leads to the formation of the rock-salt structure. However, when using a highly reactive and homogeneous co-precipitated starting powder, neither the spinel phase nor the rock-salt structure is formed, and a Co^{II}:ZnO solid solution is obtained, which remains stable up to high temperatures.

© 2008 Elsevier Inc. All rights reserved.

1. Introduction

In the last years, the emerging field of spintronics has triggered a worldwide search for new semiconductor materials with room-temperature ferromagnetic behavior [1–3]. These are the so-called dilute magnetic semiconductors (DMS) and, if accomplished, they could form the basis for charge, spin-based, or mixed spin- and charge-based devices. Although the origin of ferromagnetism in wide-band-gap semiconductors is still far from being understood, a general approach based on the mean-field theory implicitly assumes the following description for a DMS [4,5]: a more or less random alloy in which a stoichiometric fraction of the host semiconductor atoms is substituted by transition metal ions bearing a net magnetic moment. Pursuing this situation several systems have been investigated in the past decade, among which those based on ZnO doped with 3d transition-metal ions have shown the most promising results so far [6–9]. More specifically, it has been reported that the wide-band-gap semiconductor ZnO exhibits ferromagnetism with a Curie temperature (T_C) above room temperature when the oxide is doped with a few atomic percent of Co [10–12]. However, a thorough study of the literature shows that most of the results and the provided explanations are contradictory, with some reports presuming the absence of room-

temperature ferromagnetic behavior in the Co:ZnO system [13–15]. Behind this controversy, it is found that magnetism is actually very sensitive to the conditions employed for growing the DMS material. This is mainly because depending on these growing conditions, samples consisting of single-phase random alloys, nanoclusters of magnetic atoms, precipitates and second-phase formation, or a combination of these, can be obtained. For example, for the system under investigation in this contribution, Co-doped ZnO, some authors claim that the observed ferromagnetism may be due to the presence of nanometer-sized Co-metal precipitates [16–18]. Instead of that, some others suggest a carrier-mediated exchange mechanism in the ZnO matrix of a homogeneous Co^{II}:ZnO solid solution, i.e. atomic-scale dissolution of Co ions in wurtzite ZnO [15,19,20]. However, the substitution of Co²⁺ for Zn²⁺ in ZnO is difficult since under thermodynamic equilibrium the solubility of Co in zincite oxide is only around 6.5 at% at 1073 K, and then decreases with temperature [21]. Moreover, some papers claim that the equilibrium solubility of Co in ZnO might be exceeded by using non-equilibrium film growth processes [12,21,22]. However, the lack of reproducibility of the prepared ZnCoO films, even by the same deposition technique and for the same cobalt concentration, shows how difficult it is to dissolve cobalt in the ZnO matrix in a controlled way. Hence, the formation of secondary phases is also a possibility that has been taken into account: CoO is assumed to exhibit a weak ferromagnetic response [12], whereas the formation of the spinel ZnCo₂O₄ seems to decrease the possibility of ferromagnetism in this system

* Corresponding author. Fax: +34 91 7355843.

E-mail address: mpeiteado@icv.csic.es (M. Peiteado).

[23]. More recently, however, the presence of Co_3O_4 , although antiferromagnetic itself, has been invoked as the origin of the observed room-temperature ferromagnetic response [24]. But the situation is even more complex given that in air atmosphere the $\text{Co}^{\text{II}}/\text{Co}^{\text{III}}$ couple experiences several redox processes with temperature. This leads to the formation and decomposition of different compounds with different crystal structures, and this will strongly influence the diffusion behavior in the proposed DMS material.

Within this frame, it is clear that a picture of the microstructural evolution of the Co:ZnO system is still lacking. In this study, we solve this by analyzing the solid state chemistry of the Co:ZnO system as a function of temperature. The formation of solid solution, precipitates and/or second phases is investigated in terms of solid state diffusion.

2. Experimental procedure

The solid state interaction in the Zn–Co–O system is first investigated by using the well-known technique of the diffusion couples. This technique has been proved quite successful for studying the interaction between different binary, ternary and multiphase ceramic systems [25]. ZnO and CoO analytical grade chemicals (Sigma-Aldrich) were used as starting powders to prepare the pellets of the diffusion couple. Nevertheless, due to the mentioned reduction processes of the CoO compound, the initial CoO pellet is referred to as the CoO_x pellet. The preparation of the couple is described elsewhere [26]: a 20-mm-diameter base of ZnO powder was first pressed at 50 MPa; subsequently, a 6-mm-diameter pellet of CoO powder, previously pressed at 200 MPa, was placed over this base, and the die was filled with more ZnO powder till the cobalt pellet was totally covered. The whole ensemble was pressed at 250 MPa. The diffusion couple thus obtained was fired in air atmosphere at temperatures ranging from 873 to 1273 K with 12 h dwell time. Up to five samples were fired at each temperature.

Following the results of the diffusion couple analyses, the preparation of the $\text{Zn}_{0.99}\text{Co}_{0.01}\text{O}$ nominal composition was attempted by applying a highly reactive co-precipitation method. Polycrystalline samples were obtained via a single-source crystalline oxalate precursor, which ensures random atomic-scale mixing of the ions involved [15]. The precursor was obtained by room-temperature co-precipitation with oxalic acid of aqueous solutions of zinc and cobalt acetates, $\text{Zn}(\text{CH}_3\text{COO})_2 \cdot 2\text{H}_2\text{O}$ and $\text{Co}(\text{CH}_3\text{COO})_2 \cdot 4\text{H}_2\text{O}$. Reagent-grade raw materials (Sigma-Aldrich) were used in all cases. The precipitated oxalate was calcined at 673 K to cleanly decompose it into the corresponding oxide. More details about the synthesis method are described elsewhere [13]. The calcined powder was pressed into pellets and heated at temperatures ranging from 873 to 1373 K for 2 h.

The thermal evolution of the CoO raw material was followed by differential thermal analysis and thermogravimetry (DTA-TG) on a Netzsch STA 449 C instrument in air atmosphere at a heating rate of 3 K/min. Characterization of the diffusion couples and the co-precipitated samples was carried out on a Cold Field Emission-Scanning Electron Microscope (Model S-4700 Hitachi) equipped with an Energy Dispersive Spectroscopy Microanalysis Probe (EDS). The couples were fractured and the pellets were carefully separated, and problems arising with topology were overcome by the use of a double-tilt sample holder in the microscope. The thermal evolution of the co-precipitated samples was also followed by means of X-ray diffraction (XRD) using a Bruker AXS Endeavor 4 Diffractometer.

3. Results and discussion

3.1. DTA-TG and EDS analyses

DTA-TG measurements depicted in Fig. 1 show the thermal evolution in air of the raw CoO used in this study. A weight gain of approximately 6.1% is observed in the range 673–973 K, accompanied by a sharp weight loss of 6.6% when temperature increases above 1173 K. These two processes correspond to the oxidation of the starting $\text{CoO}-\text{Co}_3\text{O}_4$ and the later decomposition of this last one to give again the monoxide, respectively [27]. Both compounds exhibit well-differentiated crystal structures. EDS analyses of samples fired below 873 K show no evidence of zinc diffusing into the cobalt oxide pellet. At this temperature the oxidation of starting CoO is in progress, but no diffusion of cobalt into ZnO is detected. The first indication of reactivity takes place when the couples are treated at 973 K for 12 h. Short-range diffusion is observed in both directions at this temperature, see Fig. 2. Although a significant degree of data scattering was observed, EDS signals yield around 1–3 at% of Zn in the vicinity of the contact surface of the CoO_x pellet (already Co_3O_4 at this temperature). The Zn signal decreases with distance to the surface, and at 15 μm inside the pellet no more zinc could be detected (Fig. 2a). On the other hand, the presence of cobalt in the ZnO pellet is detected at the contact surface, and at 30 μm inside, its presence is negligible (Fig. 2b). When the firing temperature is increased to 1073 K, the diffusion of Zn into the Co_3O_4 pellet is increased. It yields around 6–8 at% of Zn at the contact surface, and now it can be detected almost 40 μm inside the cobalt oxide pellet (Fig. 3a). Similarly, the diffusion of Co into the ZnO pellet also noticeably increased at this temperature. Around 4–6 at% of Co is detected at the contact surface of the ZnO pellet. However, in this case the diffusion covers a longer range and some Co could be detected almost 500 μm inside the ZnO pellet (Fig. 3b). When firing at 1173 K, an increase in the Zn diffusion is again detected, which now extends up to 300 μm inside the CoO_x pellet. Conversely, the diffusion of cobalt into ZnO now seems to decrease. A lower amount of cobalt is detected at the contact surface and its presence is reduced to less than 50 μm from this surface (Fig. 4). Finally, after firing the couples at 1273 K for 12 h, two different behaviors are observed, see Fig. 5. On the one hand, the diffusion of zinc continues its tendency to increase and it can be detected up to 700 μm inside the CoO_x pellet. On the contrary, the diffusion of cobalt is completely inhibited at 1273 K.

To summarize these results, the data depicted in Fig. 6 represent the maximum diffusion distance as a function of temperature for the Zn and Co species into the corresponding

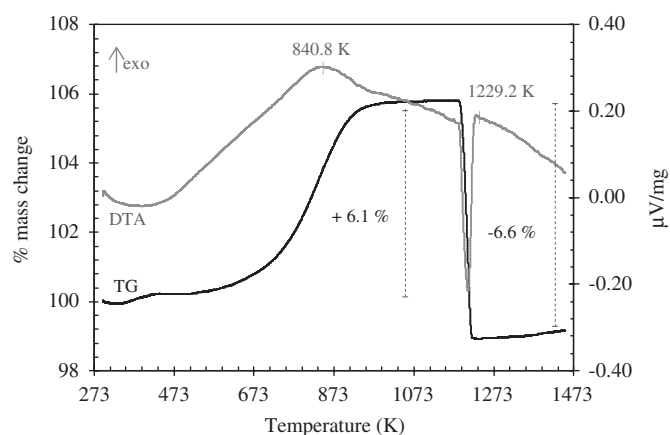


Fig. 1. DTA-TG curves for the CoO raw material used in this study.

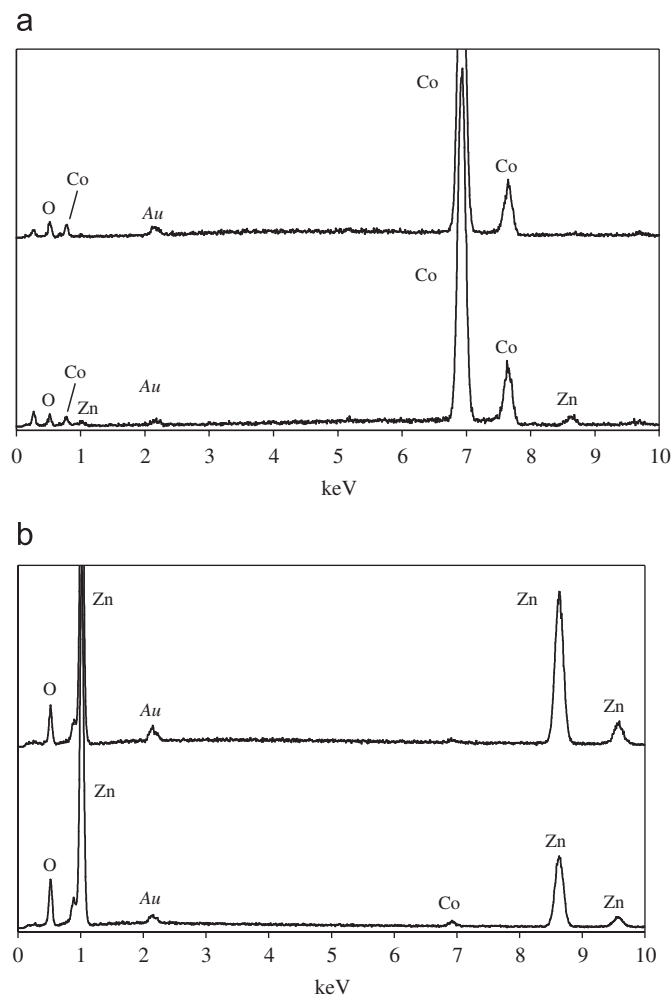


Fig. 2. EDS analyses of the couple fired at 973 K for 12 h performed at different distances from the contact surface. (a) CoO_x pellet. From below: spectra of the contact surface and 15 mm inside. (b) ZnO pellet. From below: spectra of the contact surface and 30 mm inside.

pellets of the couple. By maximum diffusion distance, we assume the distance beyond which no further diffusion is detected by EDS. As observed, two different patterns are obtained for Zn and Co species. Diffusion of Zn into the CoO_x pellet continuously increases from slight short-range diffusion at 973 K to a large range at 1273 K. Meanwhile, Co diffusion reaches a maximum at 1073 K and then continuously decreases with temperature until 1273 K, when it is completely inhibited. Furthermore, dashed lines in the plot of Fig. 6 represent the temperature values at which the transformations between CoO and Co₃O₄ compounds take place. According to this representation, it is possible to infer that the diffusion behavior in the ZnO–CoO_x system is determined by these transformations between the two cobalt oxides, especially in the case of cobalt ions going into the ZnO structure.

3.2. ZnO–CoO diffusion patterns

CoO has the rock-salt structure with Co^{II} ions in six-fold coordination. Recent studies indicate that Co^{II} ions adopt a high-spin configuration in this arrangement [28], which implies an ionic radius of 0.745 Å [29]. On the other hand, ZnO has a wurtzite structure with Zn^{II} ions in four-fold coordination and an ionic radius of 0.60 Å. The ionic radius of Co^{II} decreases to 0.58 Å in tetrahedral coordination and the ionic radius of Zn^{II} increases to

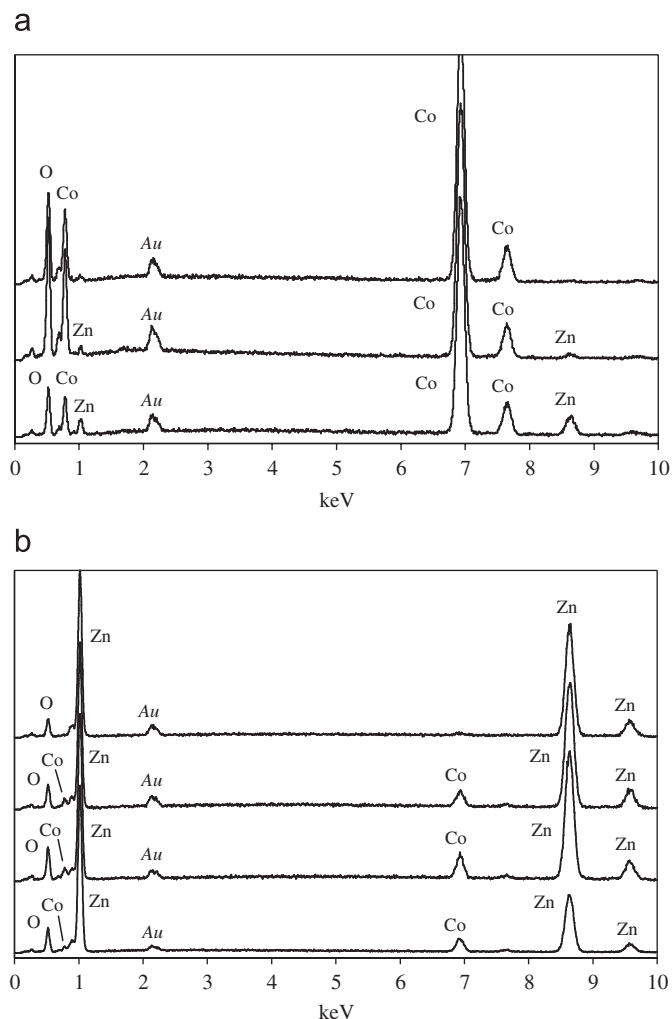


Fig. 3. EDS analyses of the couple fired at 1073 K for 12 h performed at different distances from the contact surface. (a) CoO_x pellet. From below: spectra of the contact surface, 20 mm inside and 40 mm inside. (b) ZnO pellet. From below: spectra of the contact surface, 200 mm inside, 200 mm inside and 500 mm inside.

0.74 Å when progressing to octahedral coordination [29]. At first this similarity in charge and ionic size suggests the possibility of substitutional solid solution for both the Co^{II} into the ZnO wurtzite structure and the Zn^{II} into the CoO rock-salt structure, respectively. The EDS results show that in the temperature range between 873 and 973 K, no zinc diffuses into the rock-salt structure (Fig. 6). At these low temperatures, we can assume that Zn^{II} diffusion has not been activated yet. This is confirmed by the fact that at temperatures above 1173 K, when the CoO compound is again present, the diffusion of Zn^{II} into this rock-salt structure is greatly enhanced (Fig. 6). In the case of Co^{II} ions diffusing into the wurtzite structure, the situation is however different. No diffusion of cobalt is detected in any moment from the rock-salt structure of the CoO compound or even at the high-temperature range between 1173 and 1273 K (Fig. 6). This indicates that for the Co^{II} ions to be released from the rock-salt arrangement, higher temperatures than those tested in this study are required. In other words, Co^{II} diffusion from CoO seems to show high activation energy.

3.3. ZnO–Co₃O₄ diffusion patterns

Co^{II}Co^{III}₂O₄ has the normal spinel structure with Co^{II} ions in tetrahedral and Co^{III} in octahedral sites within the cubic closest

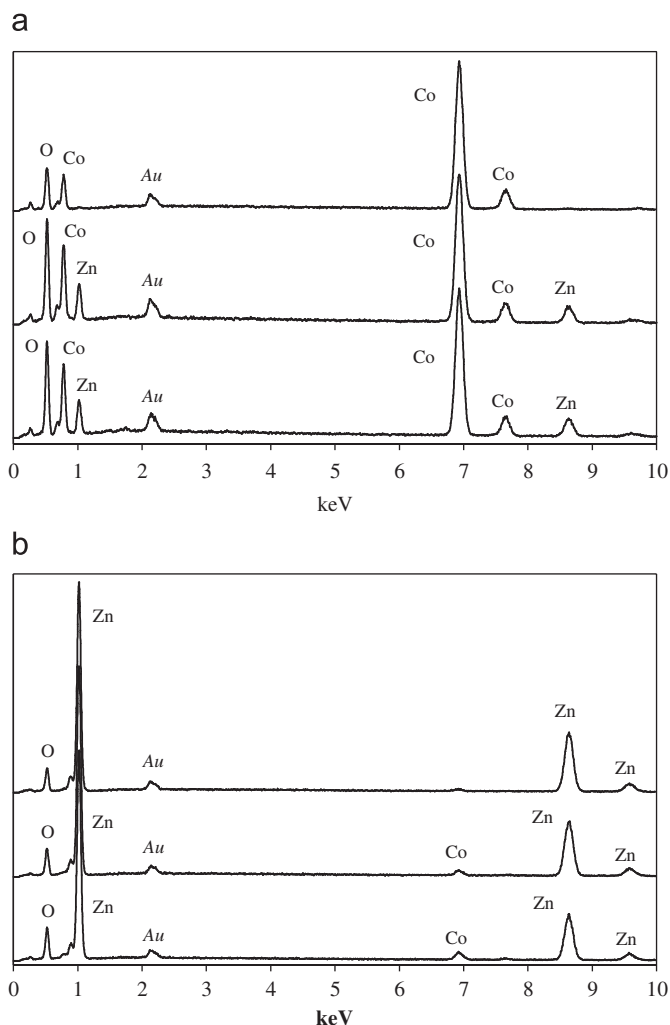


Fig. 4. EDS analyses of the couple fired at 1173 K for 12 h performed at different distances from the contact surface. (a) CoO_x pellet. From below: spectra of the contact surface, 10 mm inside and 50 mm inside. (b) ZnO pellet. From below: spectra of the contact surface, 100 mm inside and 300 mm inside.

packing (ccp) lattice of oxide ions. This is attributed to the dominating advantage of placing the d⁶ ions in octahedral sites, where adoption of the low-spin configuration gives it a decisively favorable crystal field stabilization energy [30]. Consequently, the ionic radii of the cobalt species in the spinel structure are 0.58 and 0.545 Å for the Co^{II} and Co^{III} ions, respectively [29]. As mentioned, the ionic radius of Zn^{II} in four-fold coordination is 0.60 Å; hence, Zn^{II} ions could feasibly substitute the Co^{II} ions in the tetrahedral positions of the spinel arrangement. This is confirmed by an increased diffusion of Zn species in the range 973–1173 K (Fig. 6). With regard to cobalt diffusion, there is no evidence of Co^{III} ions being stable in tetrahedral coordination [29]; hence, the possibility of Co:ZnO solid solution is restrained to the diffusion of Co^{II} ions into the wurtzite tetrahedral positions. The results show that now, contrary to the rock-salt structure, cobalt ions can easily leave the spinel arrangement and diffuse into the ZnO pellet (Fig. 6).

Therefore, whereas the diffusion of zinc ions into the CoO_x pellet is simply determined by the usual thermodynamic and kinetics requirements, the diffusion of cobalt into ZnO strongly depends on the crystal structure of the starting cobalt oxide. The Co:ZnO solid solution, actually Co^{II}:ZnO solid solution, could only be achieved once the Co₃O₄ phase is formed. It has subsequently a limited stability: as the Co^{III}–Co^{II} reduction process progresses, the

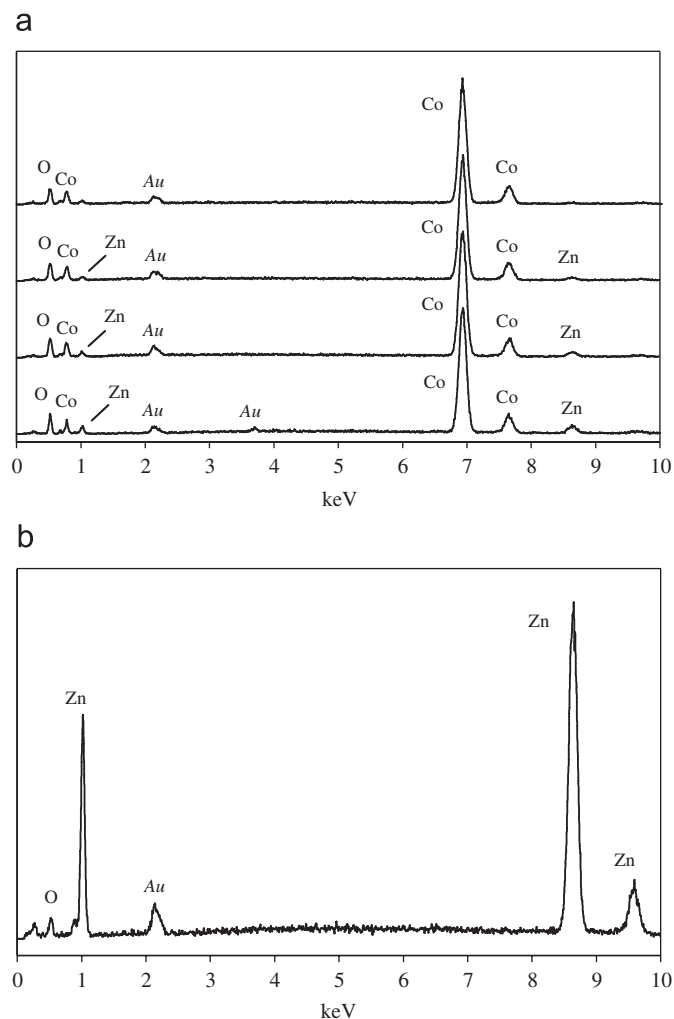


Fig. 5. EDS analyses of the couple fired at 1273 K for 12 h performed at different distances from the contact surface. (a) CoO_x pellet. From below: spectra of the contact surface, 50 mm inside, 200 mm inside and 700 mm inside. (b) ZnO pellet, spectra of the contact surface.

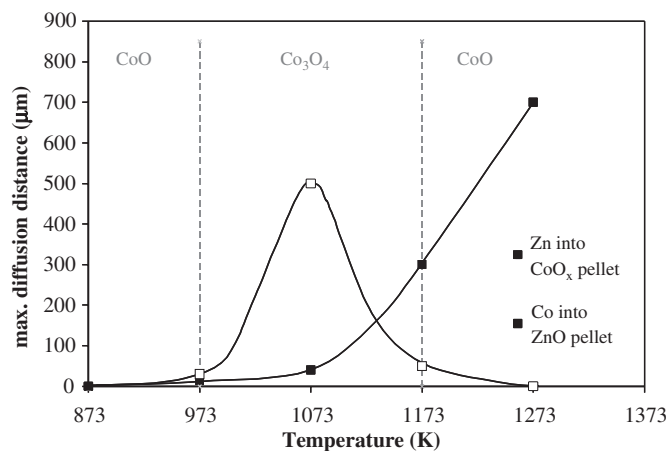


Fig. 6. Maximum diffusion distance for the ZnO–CoO_x couple as a function of temperature. Dashed gray lines represent the temperature values at which the transformations between CoO and Co₃O₄ compounds take place.

rock-salt structure is again formed and from this structure, within the range of temperatures studied in this work, the diffusion of the Co^{II} ions is not possible. Besides, there is another interesting

result that can be extracted from EDS analyses: in these samples the postulated formation of the ZnCo_2O_4 spinel phase [23] was never observed for the whole range of tested temperatures. Nor was it detected at the contact surface of the pellets (the formation of a spinel phase has been observed in analogous systems prepared by solid state, meaning Zn–Mn–O [26,31,32]). According to these results, increasing the reactivity of the system might be critical in obtaining reliable $\text{Co}^{\text{II}}:\text{ZnO}$ solid solution materials. As is well known, an increased degree of reactivity is achieved when the ceramic powders are prepared from chemical precursors of the involved Zn^{II} and Co^{II} cations. In this sense, we attempt the use of a highly reactive co-precipitation synthesis to analyze the microstructural evolution of the $\text{Zn}_{1-x}\text{Co}_x\text{O}$ system.

3.4. $\text{Zn}_{1-x}\text{Co}_x\text{O}$ co-precipitated samples

As mentioned in the Experimental procedure, this part of the work was carried out by applying an oxalate-precursor co-precipitation method to obtain polycrystalline samples of the $\text{Zn}_{0.99}\text{Co}_{0.01}\text{O}$ nominal composition. The as-precipitated powder was calcined at 673 K for 4 min, leading already to a homogeneous soft green coloration of the sample. This powder was initially characterized on the microscope (FE-SEM). As can be seen in Fig. 7, a fine homogeneous nanometer-sized powder without clusters of secondary phases (spinel phase, rock-salt) is obtained. Although qualitative, EDS analyses of this powder reveal the presence of cobalt all around the sample. Pellets of the calcined powder were then pressed and sintered. For the whole range of tested temperatures, XRD spectra of the heated pellets showed only peaks corresponding to the ZnO wurtzite (not depicted here), without any secondary phase being detected by this technique. Fig. 8 shows the FE-SEM micrograph of the sample treated at 1373 K for 2 h. No secondary phases are detected in this sample and the EDS analyses on polished surface yield 1 at% of Co inside the ZnO grains, evidencing the existence of the $\text{Co}^{\text{II}}:\text{ZnO}$ solid solution, see Fig. 8. From these results we can infer that in the co-precipitated samples, the formation of the CoO rock-salt structure from the Co^{II} precursor is inhibited in the range of temperatures tested in this study. Instead, the Co^{II} ions diffuse inside the wurtzite structure at lower temperatures, no segregation of Co^{III} ions to the grain boundaries is observed, no spinel phase (whatever ZnCo_2O_4 or Co_3O_4) is thus formed and the subsequent transformation to the rock-salt structure is therefore avoided, hence a stable $\text{Co}^{\text{II}}:\text{ZnO}$ solid solution can be obtained up to a high temperature.

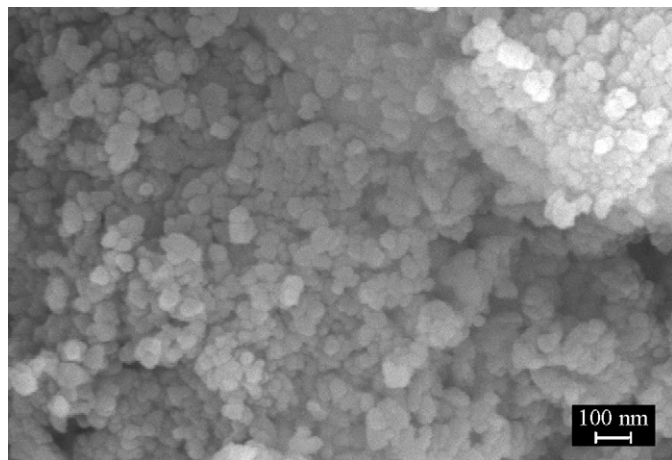


Fig. 7. FE-SEM micrograph of co-precipitated powder of nominal composition $\text{Zn}_{0.99}\text{Co}_{0.01}\text{O}$ after calcination at 673 K for 4 min.

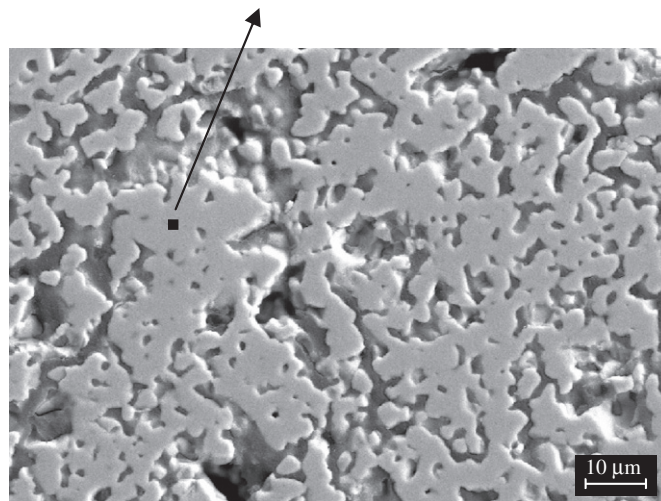
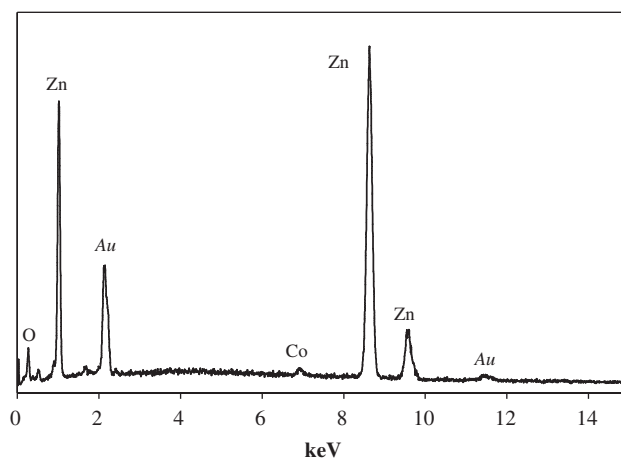


Fig. 8. FE-SEM micrograph and EDS analysis of co-precipitated powder of nominal composition $\text{Zn}_{0.99}\text{Co}_{0.01}\text{O}$ treated at 1373 K for 2 h.

4. Conclusions

The analysis of the solid state interaction in the $\text{Zn}_{1-x}\text{Co}_x\text{O}$ nominal system reveals that the formation of a homogeneous $\text{Co}:\text{ZnO}$ solid solution is determined by the crystal structure from which Co^{II} ions diffuse into the wurtzite lattice. No diffusion is observed whenever the CoO rock-salt structure is formed from the Co^{II} precursor. From the Co_3O_4 spinel phase, the diffusion is feasible but has a limited temperature range defined by the reduction at a high temperature of $\text{Co}^{\text{III}}-\text{Co}^{\text{II}}$, since this process again leads to the formation of the rock-salt. However, when a highly reactive co-precipitation method is used, no spinel phase is formed and the subsequent transformation to the rock-salt structure is therefore avoided. Instead a $\text{Co}^{\text{II}}:\text{ZnO}$ solid solution is achieved at the temperature of calcinations, which remains stable up to high temperatures.

Acknowledgments

The authors would like to express their gratitude to the Ministry of Higher Education, Science and Technology of Slovenia for its financial support. Dr. Peiteado also acknowledges the Secretaría de Estado de Universidades e Investigación del Ministerio de Educación y Ciencia (Spain) for the financial support. This work has been conducted within the CICYT MAT 2007-66845-C02-01 and CICYT MAT 2007-65857 projects.

References

- [1] S.J. Pearton, C.R. Abernathy, M.E. Overberg, G.T. Thaler, D.P. Norton, N. Theodoropoulou, A.F. Hebard, Y.D. Park, F. Ren, J. Kim, L.A. Boatner, *J. Appl. Phys.* 93 (2003) 1.
- [2] S.A. Wolf, D.D. Awschalom, R.A. Buhrman, J.M. Daughton, S. Von Molnar, M.L. Roukes, A.Y. Chtchelkanova, D.M. Treger, *Science* 294 (2001) 1488.
- [3] H. Ohno, *Science* 281 (1998) 951.
- [4] S.J. Pearton, W.H. Heo, M. Ivill, D.P. Norton, T. Steiner, *Semicond. Sci. Technol.* 19 (2004) R59.
- [5] C. Liu, F. Yun, H. Morkoc, *J. Mater. Sci. Mater. **El.* 16 (2005) 555.
- [6] Ü. Özgür, Y.I. Alivov, C. Liu, A. Teke, M.A. Reshchikov, S. Dogan, V. Avrutin, S.J. Cho, H. Morkoc, *J. Appl. Phys.* 98 (2005) 1.
- [7] T. Dietl, H. Ohno, *Science* 287 (2000) 1019.
- [8] K. Sato, H. Katayama-Yoshida, *Physica E* 10 (2001) 251.
- [9] W. Prellier, A. Fouchet, B. Mercey, *J. Phys. Condens. Mater.* 15 (2003) R1583.
- [10] C.B. Fitzgerald, M. Venkatesan, J.G. Lunney, L.S. Dorneles, J.M.D. Coey, *Appl. Surf. Sci.* 247 (2005) 493.
- [11] H.J. Lee, S.Y. Jeong, C.R. Cho, C.H. Park, *Appl. Phys. Lett.* 81 (2002) 4020.
- [12] K. Ueda, H. Tabata, T. Kawai, *Appl. Phys. Lett.* 79 (2001) 988.
- [13] M. Bouloudenine, N. Viart, S. Colis, A. Dinia, *Chem. Phys. Lett.* 397 (2004) 73.
- [14] M. Bouloudenine, N. Viart, S. Colis, J. Kortus, A. Dinia, *Appl. Phys. Lett.* 87 (2005) 052501.
- [15] G. Lawes, A.S. Risbud, A.P. Ramirez, R. Seshadri, *Phys. Rev. B.* 71 (2005) 1.
- [16] J.H. Park, M.G. Kim, H.M. Jang, S. Ryu, Y.M. Kim, *Appl. Phys. Lett.* 84 (2004) 1338.
- [17] D.P. Norton, M.E. Overberg, S.J. Pearton, K. Pruessner, J.D. Budai, L.A. Boatner, M.F. Chisholm, J.S. Lee, Z.G. Khim, Y.D. Park, R.G. Wilson, *Appl. Phys. Lett.* 83 (2003) 5488.
- [18] J.H. Kim, H. Kim, D. Kim, Y. Ihm, W.K. Choo, *J. Eur. Ceram. Soc.* 24 (2004) 1847.
- [19] K. Rode, A. Anane, R. Mattana, J.P. Contour, O. Durand, R. LeBourgeois, *J. Appl. Phys.* 93 (2003) 7676.
- [20] A.S. Risbud, N.A. Spaldin, Z.Q. Chen, S. Stemmer, R. Seshadri, *Phys. Rev. B.* 68 (2003) 2052021.
- [21] L. Poul, S. Ammar, N. Jouini, F. Fievet, F. Villain, *Solid State Sci.* 3 (2001) 31.
- [22] S. Deka, R. Pasricha, P.A. Joy, *Chem. Mater.* 16 (2004) 1168.
- [23] A. Quesada, M.A. García, M. Andrés, A. Hernando, J.F. Fernández, A.C. Caballero, M.S. Martín-González, F. Briones, *J. Appl. Phys.* 100 (2006) 113909.
- [24] J. Blasco, F. Bartolomé, L.M. García, J. García, *J. Magn. Magn. Mater.* 316 (2007) e177.
- [25] D. Makovec, D. Kolar, M. Trontelj, *Mater. Res. Bull.* 28 (1993) 803.
- [26] M. Peiteado, A.C. Caballero, D. Makovec, *J. Solid State Chem.* 180 (2007) 2459.
- [27] C.B. Wang, H.K. Lin, C.W. Tang, *Catal. Lett.* 94 (2004) 69.
- [28] S.C. Petitto, M.A. Langell, *Surf. Sci.* 599 (2005) 27.
- [29] R.D. Shannon, *Acta Cryst. A* 32 (1976) 751.
- [30] N.N. Greenwood, A. Earnshaw, *Chemistry of the Elements*, Pergamon Press, Oxford, 1984, pp. 1211–1241.
- [31] J. Blasco, J. García, *J. Solid State Chem.* 179 (2006) 2199.
- [32] M. Peiteado, S. Sturm, A.C. Caballero, D. Makovec, *Acta Mater.* doi:10.1016/j.actamat.2008.04.024.